*Catalysis Letters Vol. 100, Nos. 3–4, April 2005 (© 2005)*
DOI: 10.1007/s10562-004-3440-y


# Electrochemical promotion of $RuO_2$ catalysts for the combustion of toluene and ethylene

I. Constantinou[a], I. Bolzonella[b], C. Pliangos[a], Ch. Comninellis[b], and C. G. Vayenas[a,*]

[a]*Department of Chemical Engineering, University of Patras, Patras, GR 26504, Greece*
[b]*Institute of Chemical Engineering, Swiss Federal Institute of Technology, CH-1015, Lausanne, Switzerland*

Received 27 September 2004; accepted 11 December 2004

The electrochemical promotion of the complete catalytic oxidation of ethylene and toluene on $RuO_2$Catalyst films deposited on $Y_2O_3$-stabilized-$ZrO_2$ (YSZ) has been investigated at temperatures 400 to 500 °C. Anodic polarization (1.5 V), i.e. $O^{2-}$ supply from the YSZ support to the catalyst, is found to enhance the rates of ethylene and toluene oxidation by a factor of 10 and 8 respectively. Cathodic polarization (−1.5 V) i.e. oxygen removal from the catalyst, enhances the oxidation rates by a factor of 3 and 4, respectively. These rate enhancements are strongly nonFaradaic. The kinetics, positive order in both reactants, and the promotional results, inverted-volcano type for both reactions, conform to the recently found rules of electrochemical promotion.

**KEY WORDS:** ethylene oxidation; toluene oxidation; $RuO_2$; Yttria-stabilized zirconia; electrochemical promotion.

## 1. Introduction

The catalytic activity and selectivity of porous metal films interfaced with solid electrolyte supports can be altered dramatically and in a reversible manner via potential or current application between the metal catalyst-electrode and an inert counter electrode also deposited on the solid electrolyte (figure 1). The observed increase in catalytic rate can be up to five orders of magnitude higher than the rate of ion transport to or from the solid electrolyte [1–15].

Recent work has shown that electrochemical promotion results from electrochemically controlled migration of promoting ionic species ($O^{\delta-}$, $Na^{\delta+}$) from the electrolyte support to the metal/gas catalytic interface where an "effective" double layer is formed (figure 1, bottom) [9,13,14] and that classical promotion, electrochemical promotion and metal–support interactions with $O^{2-}$ conducting and mixed ionic-electronic conducting supports are functionally identical and only operationally different [14,16]. Electrochemical promotion allows for *in situ* control of catalyst activity and selectivity by controlling *in situ* the promoter coverage via potential application [1–17].

On application of electrical current, $I$, or potential ($\pm 2$ V) between the catalyst-electrode and a catalytically inert counter electrode, also deposited on the solid electrolyte, ionic species are supplied to the catalyst at a rate $I/(n\mathrm{F})$, where $n$ is the ion charge in the solid electrolyte support. The electrochemically generated ionically bonded promoting species migrate (backspillover) over the entire gas-exposed catalyst-electrode surface and establish an effective double layer at the catalyst/gas interface [18–21]. Each backspillover species is accompanied by its compensating (image) charge in the metal so that the effective double layer is overall neutral, [18–22]. Under these conditions, the work function, $\Phi$, of the gas-exposed catalyst-electrode surface changes with catalyst potential, $U_{\mathrm{WR}}$, in an one-to-one manner [1,13,14,22]:

$$\Delta\Phi = e\Delta U_{\mathrm{WR}} \tag{1}$$

where $\Delta U_{\mathrm{WR}}$ is the (ohmic-drop-free) change in the catalyst (working)-electrode potential $U_{\mathrm{WR}}$ with respect to the reference electrode [1,13,14,21,22]. The change in $\Phi$ is brought about at the molecular level via the above mentioned electrochemically controlled ion migration at the catalyst/gas interface.

The electrochemically controlled migration (backspillover) of promoting species has been confirmed using a variety of surface spectroscopic and electrochemical techniques including X-ray photoelectron spectroscopy (XPS) [23,24], ultraviolet photoelectron spectroscopy (UPS) [25], temperature-programmed desorption (TPD) [26], cyclic voltammetry [23,27], impedance spectroscopy [28,29], scanning tunneling microscopy STM [30,31] and work function measurements [1,19,32].

Two parameters are commonly used to describe the magnitude of electrochemical promotion:

1. The apparent Faradaic efficiency, $\Lambda$, defined from:

$$\Lambda = \Delta r_{\mathrm{catalytic}}/(I/2F) \tag{2}$$

* To whom correspondence should be addressed.
E-mail: cat@chemeng.upatras.gr

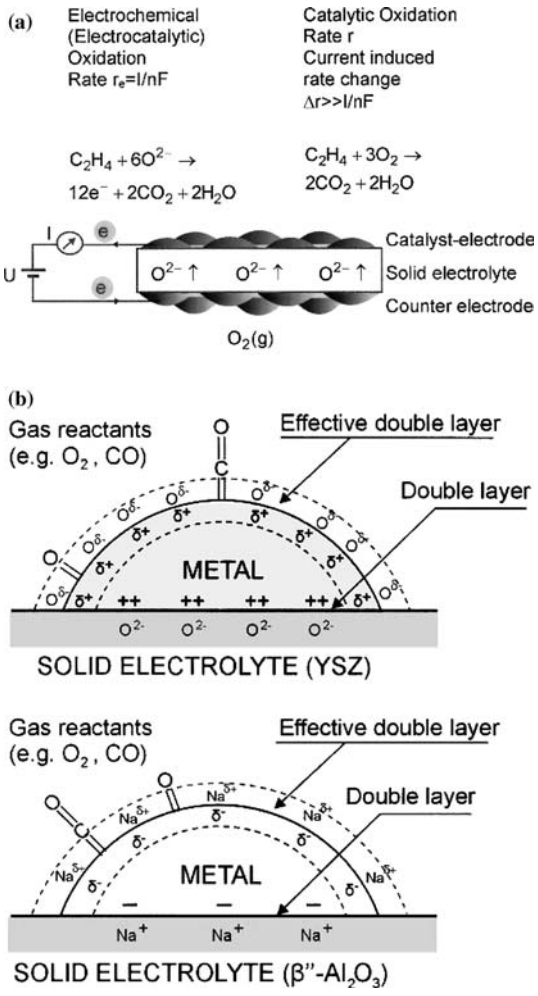


Figure 1. (a) Principle and basic experimental setup for electrochemical promotion (NEMCA) studies using an $O^{2-}$-conducting solid electrolyte. (b) Schematic representation of a metal catalyst-electrode deposited on an $O^{2-}$-conducting electrolyte and a $Na^+$-conducting solid electrolyte, showing the location of the metal-solid electrolyte double layer and of the effective double layer created at the metal/gas interface due to potential-controlled ion migration (backspillover).

where $\Delta r_{catalytic}$ is the current- or potential-induced change in catalytic rate, $I$ is the applied current and F is Faraday's constant.

2. The rate enhancement, $\rho$, defined from:

$$\rho = r/r_0 \quad (3)$$

where $r$ is the electropromoted catalytic rate and $r_o$ is the unpromoted (open-circuit) catalytic rate.

A reaction exhibits electrochemical promotion when $|\Lambda| > 1$, while electrocatalysis is limited to $|\Lambda| \leq 1$. A reaction is termed electrophobic when $\Lambda > 1$ and electrophilic when $\Lambda < -1$. In the former case the rate increases with catalyst potential, $U_{WR}$, while in the latter case the rate decreases with catalyst potential. $\Lambda$ values up to $3 \times 10^5$ [1,13,14] and $\rho$ values up to 150 [14] have been found for several systems.

Recent work has identified simple and rigorous rules which permit the prediction of the rate dependence on catalyst potential, $U_{WR}$, and work function $\Phi$ and thus allow for the prediction of the sign of $\Lambda$ on the basis of the unpromoted kinetics [14,33].

In this work, a $RuO_2$ polycrystalline film deposited on a ceramic solid electrolyte $Y_2O_3$-stabilized $ZrO_2$ (YSZ), was used as the catalyst for the combustion of ethylene and toluene. Ethylene and toluene were chosen as probe molecules of volatile organic compounds. Alkenes and aromatics are the majority of organic pollutants in automobile exhausts and numerous industrial processes. The group of Comninellis has already demonstrated the electrochemical promotion of such thin $RuO_2$ and $IrO_2$ metal oxide films for the gas phase combustion of ethylene [34–38].

## 2. Experimental

The electrochemical promotion of ethylene and toluene oxidation was investigated on porous and electrically continuous $RuO_2$ films deposited on YSZ (figure 2 bottom). The $RuO_2$ film serves simultaneously as the oxidation catalyst and as the working (W) electrode of the solid electrolyte cell:

$$C_7H_8/C_2H_4, O_2, \text{ products }, RuO_2| \text{ YSZ } | \text{ Au},$$
$$C_7H_8/C_2H_4, O_2, \text{ products}$$

where the working $RuO_2$ electrode and the Au counter and reference electrodes are all exposed to the same reaction mixture (figure 2).

This type of reactor is known as "single pellet" reactor [14]. It has a volume of ~30 $cm^3$ and under the experimental conditions used in the present study it behaves as a continuous stirred tank reactor (CSTR). More details can be found elsewhere [13,14,22,26]. The reaction temperature is monitored via a thermocouple (type K) in contact with the YSZ surface.

The YSZ solid electrolyte was a thin rectangular plate (20 mm × 10 mm and 1 mm thickness) of 8 mol% $Y_2O_3$-stabilized-$ZrO_2$ (YSZ) (METOXIT AG.). The geometrical area of the working electrode was ~50 $mm^2$ (7 mm × 7 mm) while those of the reference and counter electrodes were ~7 $mm^2$ (1 mm × 7 mm) and ~50 $mm^2$ (7 mm × mm), respectively.

Gold paste counter and reference electrodes (Gwent Electronic Materials Ltd.) were deposited on the one side of the solid electrolyte plate via deposition of a thin paste layer followed by calcination at 550 °C. Blank experiments showed that the catalytic activity of the thus deposited Au electrodes was practically negligible in comparison with that of the $RuO_2$ Catalyst for both oxidation reactions.

The $RuO_2$ polycrystalline film (working electrode) was deposited on the other side of the plate using the thermal decomposition technique [34]. According to this technique the precursor, usually a salt, is diluted in the proper solvent (water, ethanol, isopropanol etc.). Then,

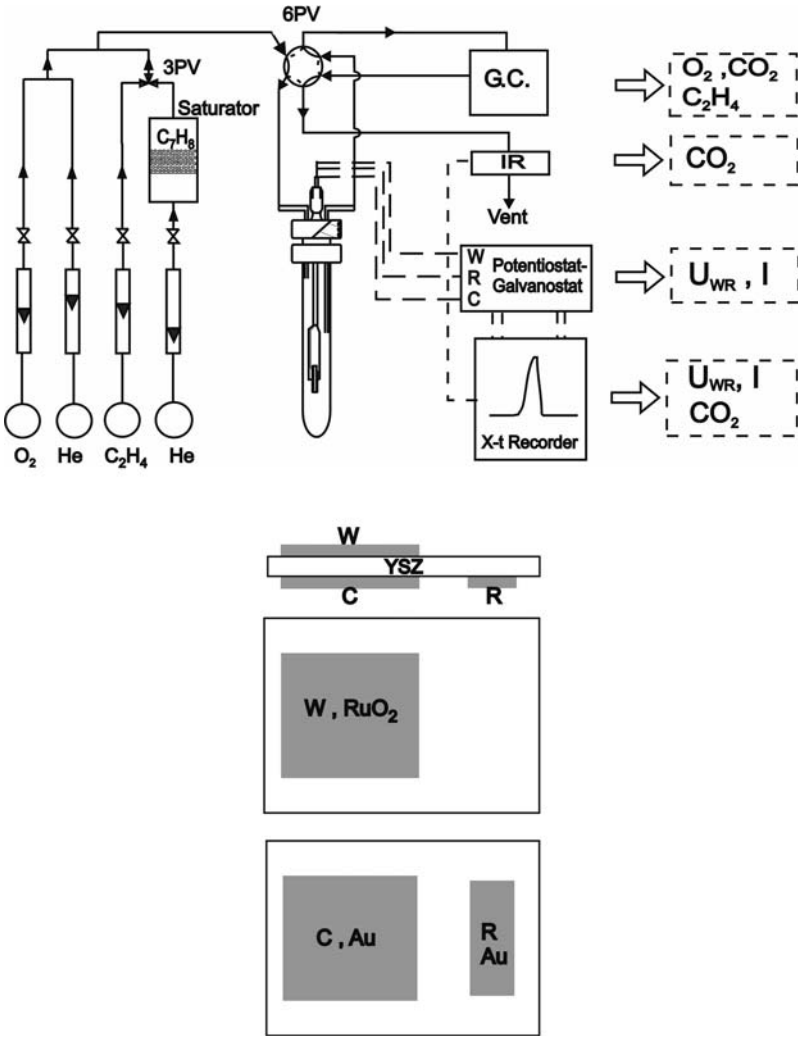


Figure 2. Schematic of the experimental setup (top) and of the YSZ plate (bottom) showing the geometry of the working (W), counter (C) and reference (R) electrodes.

via a micropipette, a proper quantity of the solution is applied on the pre-heated solid electrolyte surface. The sample is dried at a temperature slightly above the boiling point of the solvent to guarantee a fast but not instantaneous evaporation of the solvent. At last, the sample is calcined at high temperature. In our case, 3 $\mu$l of the solution containing the precursor (0.121 M $RuCl_3$ in isopropanol) was applied on the solid electrolyte followed by drying (80 °C) and calcining in air for 1 h at 500 °C. After the end of this procedure only $RuO_2$ is formed on the solid electrolyte surface [34]. The mass of the $RuO_2$ Catalyst-electrode was 48.3 $\mu$g. The true surface area, (expressed in surface mol $RuO_2$, $N_{RuO_2}$), was estimated from the time constant $\tau$ of the catalytic rate transients, during galvanostatic transients via the expression [13,14]:

$$\tau = 2FN_{RuO_2}/I \quad (4)$$

which has been found to hold for practically all previous electrochemical promotion studies [13,14]. The thus estimated $N_{RuO_2}$ value was $5 \times 10^{-7}$ mol $RuO_2$. This value has been used, in conjunction with the measured catalytic reaction rates, to compute the turnover frequency (TOF) of the oxidation reactions.

The experimental apparatus utilizes online gas-chromatography (Varian Star 3800) and infrared spectroscopy (Anarad AR-500 series) for continuous analysis of the reactor feed and products. The gas chromatograph was equipped with two detectors (a Thermal Conductivity Detector, TCD and a Flame Ionisation Detector, FID) and two columns, a CTR-I column (Porapak Q and MS5A) and a capillary column (Cp-Sil 8CB, ID 0.53 mm, 50 m length). The infrared analyser was used to monitor the $CO_2$ Concentration in the effluent stream. Its signal was recorded on a three-channel pen recorder (YOKOGAWA HOKUSHIN ELECTRIC, type 3066). Certified Oxygen (Air Liquide), Ethylene (Air Liquide) and Toluene (MERCK) placed in a thermostatted saturator were diluted in ultrapure He (99.999%, Air Liquide) (figure 2). A galvanostat-potensiostat (Amel Instruments, model 2053) was used for constant current or potential application, i.e. for galvanostatic or potentiostatic

operation. Under the temperature and gas composition conditions of the present investigation, $CO_2$ and $H_2O$ were the only detectable oxidation products. The conversion of both ethylene and toluene was kept below 15% to maintain differential reactor conditions. Carbon mass balance closure was within 5–10%.

## 3. Results and discussion

### 3.1. Ethylene oxidation

The case of the complete ethylene oxidation

$$C_2H_4 + 3O_2 \rightarrow 2CO_2 + 2H_2O \quad (5)$$

was examined first on the $RuO_2$Catalyst-electrode.

The experiments were carried out in the temperature range 400–450 °C and for $P_{O_2}/P_{C_2H_4}$ ratios between 0.35 and 35. The total flowrate was between 140 and 200 $cm^3$ (STP)/min.

Figure 3 shows a typical galvanostatic NEMCA experiment. It shows the transient effect of constant positive current application on the rate of formation of $CO_2$ and on the catalyst potential $U_{WR}$. The experiment was carried out at fixed feed gas composition, i.e., $P_{O_2} = 0.9$ kPa and $P_{C_2H_4} = 2.2$ kPa at 430 °C.

Initially, for $t < 0$, the circuit is open (o.c.) and the steady-state rate of $C_2H_4$ oxidation to $CO_2$ is equal to $1.83 \times 10^{-8}$ mol O/s. At $t = 0$, a constant anodic current, ($I = 200$ $\mu$A) is applied between the catalyst and the counter electrode. Oxygen ions, $O^{2-}$, are transferred from the YSZ support to the $RuO_2$ catalyst-electrode at a rate $I/2F$ equal to $1.03 \times 10^{-9}$ mol O/s, where F is the Faraday constant. At the same time the rate of $C_2H_4$ oxidation to $CO_2$ increases and after 70 min approaches a new steady state ($r = 19.4 \times 10^{-8}$ mol O/s). The increase in the catalytic rate $\delta r$ ($= 1.76 \times 10^{-7}$ mol O/s) is 170 times greater than the rate of ion transport, $I/2F$. A 10-fold rate enhancement ($\rho = 11$) is observed. After current interruption the catalytic rate of $CO_2$ formation returns to its initial open circuit (o.c.) value showing the reversibility of the phenomenon.

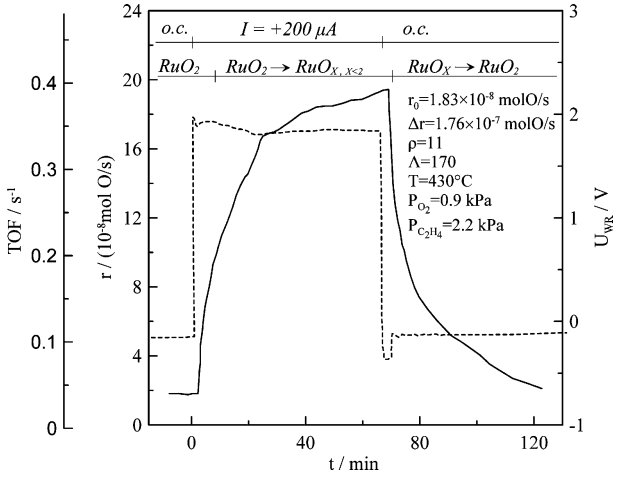


Figure 3. Transient effect of a constant positive applied current (+200 $\mu$A) on the rate of $CO_2$ production and on the catalyst potential. $T = 430$ °C, $P_{O_2} = 0.9$ kPa, $P_{C_2H_4} = 2.2$ kPa.

It is also interesting to notice in figure 3 the catalyst potential response (dashed line). Initially, when the current is applied via the galvanostat, the potential reaches the value of 2 V and gradually decreases, approaching a final steady state value of 1.8 V. The inverse behaviour is observed during current interruption: The potential is quite negative (~−250 mV), lower than that of the initial open circuit value and is then abruptly restored to its initial value. This behaviour indicates a change in the oxidation state of the catalyst surface. The gradual decrease in catalyst potential during anodic polarization indicates that $RuO_2$ is somehow reduced (lower potential) forming an oxide of the type ($RuO_x$, $x < 2$) according to the reaction:

$$RuO_2 \rightarrow RuO_x + ((2 - x)/2)O_2 \quad (6)$$

Former studies of the same reaction on Rh catalyst films have shown that application of currents or potentials can affect significantly and in a reversible manner the stability limits of surface Rh oxide, thus affecting the catalytic activity in a pronounced manner [14,33,39,40].

Steady state measurements were carried out under open circuit conditions and under anodic and cathodic polarization. Figure 4 shows the effect of catalyst potential on the catalytic rate at temperatures 400–450 °C. At 400 °C the catalytic rate increases monotonically with potential or, equivalently, with catalyst work function, ($\Delta\Phi = e\Delta U_{WR}$, equation (1)) [13,14,22], i.e. the reaction exhibits purely electrophobic behaviour ($\partial r/\partial\Phi > 0$) [13,14]. According to the recently established rules of electrochemical promotion [14,33] this type of behaviour is obtained when the electron acceptor reactant (O) is more strongly adsorbed on the catalyst surface than the electron donor ($C_2H_4$) reactant. This behaviour changes at higher temperatures where a rate enhancement is observed for both anodic and cathodic polarization. This behaviour is known as *inverted volcano behaviour* and according to the recently identified rules of electrochemical promotion [14,33] it is observed when both the electron donor ($C_2H_4$) and the electron acceptor (O) reactants are absorbed weakly on the catalyst surface, i.e. when they are both present on the catalyst surface at low coverages. This is consistent with the present observation, i.e. that inverted volcano behaviour is observed at the higher temperatures investigated.

As shown by the straight lines in figure 4, over a narrow potential range the catalytic rate dependence on catalyst potential $U_{WR}$ is described by the frequently reported equation of electrochemical promotion [13,14]:

$$\ln(r/r_0) = \frac{\alpha F \Delta U_{WR}}{RT} = \frac{\alpha \Delta\Phi}{k_b T} \quad (7)$$

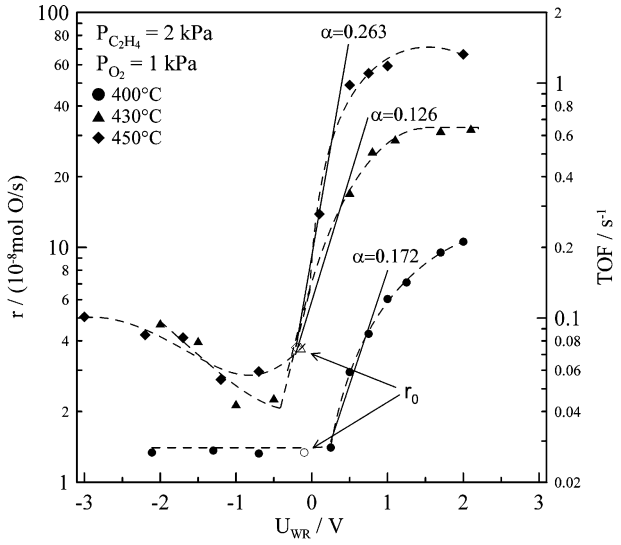


Figure 4. Effect of catalyst potential on the rate of $C_2H_4$ oxidation on $RuO_2$/YSZ.

where α is the electropromotion coefficient, positive for electrophobic reactions, negative for electrophilic ones [13,14], taking values of the order of 0.2 in the present case. Typically α is of the order 0.1–1 for electrophobic reactions and −0.1 to −1 for electrophilic reactions [13,14].

Figure 5 shows the steady state effect of positive or negative applied current $I$ or, equivalently rate of $O^{2-}$ ion transfer to/from the catalyst ($I/2F$), on the observed increase in the total rate of oxygen consumption due to the electropromotion of the catalytic reaction. The solid lines in the figure are constant Faradaic efficiency, Λ, lines. The observed values of Λ are typically of the order of $10^2$–$10^3$ for anodic operation ($I>0$) and −10 for cathodic operation ($I<0$).

Figures 6 and 7 show the rate dependence on $P_{O_2}$ (figure 6) and on $P_{C_2H_4}$ (figure 7) under open-circuit and under positive and negative applied potential. The kinetics are always positive order in $C_2H_4$ (figure 7) and also positive order in $O_2$ for $P_{O_2}$ values below 4 kPa (figure 6) gradually changing to a zero-order dependence at higher $P_{O_2}$ values. These observations indicate weaker chemisorption of the electron donor $C_2H_4$ than of the electron acceptor oxygen on the catalyst surface and are consistent, via the recently established promotional rules [33], with the observed electrophobic behaviour (figure 4) changing to inverted volcano behaviour at higher temperatures (figure 4) where both reactants are at lower surface coverages. According to these promotional rules [33] a reaction exhibits purely electrophobic behaviour when the kinetics are positive order in the electron donor reactant and zero or negative order in the electron donor reactant. For the gaseous composition of figure 4 ($P_{C_2H_4}=2$ kPa, $P_{O_2}=1$ kPa) the rate at 430 °C is positive order with respect both to $P_{O_2}$ and $P_{C_2H_4}$ (figures 6 and 7) and thus inverted volcano behaviour is observed for 430 °C in figure 4. At lower temperatures (e.g. 400 °C) where the rate becomes nearly zero order in $O_2$, purely electrophobic behaviour is observed (figure 4, $T=400$ °C).

### 3.2. Toluene oxidation

The complete oxidation of toluene

$$C_7H_8 + 9CO_2 \rightarrow 7CO_2 + 4H_2O \qquad (9)$$

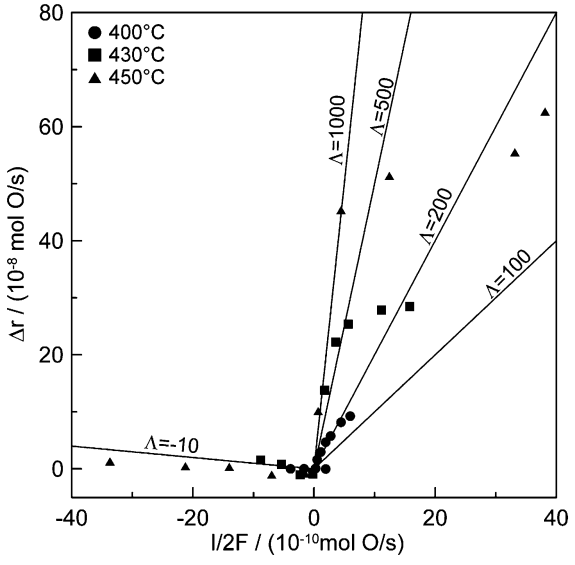


Figure 5. Effect of the applied current, I, on the rate of ethylene oxidation. $P_{C_2H_4}=2$ kPa, $P_{O_2}=1$ kPa.

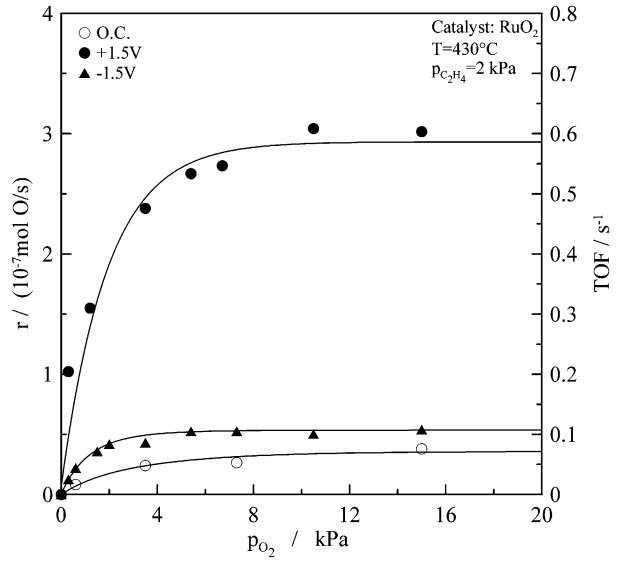


Figure 6. Effect of Oxygen partial pressure on the rate of $C_2H_4$ oxidation on $RuO_2$/YSZ under open circuit and under anodic and cathodic polarization. $P_{C_2H_4}=2$ kPa.

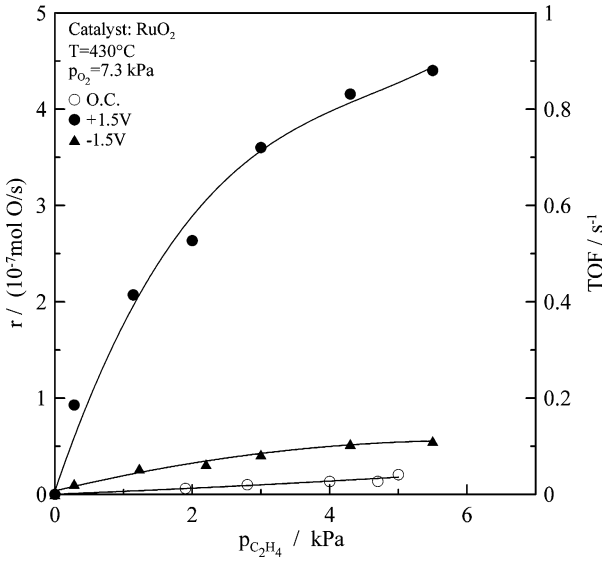


Figure 7. Effect of ethylene partial pressure on the rate of ethylene oxidation on $RuO_2$/YSZ under open circuit and under anodic and cathodic polarization. $P_{O_2} = 7.5$ kPa.

was also examined over the same $RuO_2$/YSZ catalyst surface.

Figure 8 shows an anodic galvanostatic transient experiment and figure 9 presents a similar cathodic polarization experiment, both at 450 °C and under oxidizing gaseous composition ($P_{O_2} = 7.5$ kPa and $P_{C_7H_8} = 0.2$ kPa). At anodic polarization a 800% increase in the catalytic rate of $CO_2$ formation is observed ($\rho = 9$) while under cathodic polarization (figure 9) the rate enhancement is less pronounced ($\rho = 4$). In both cases the $\Lambda$ values (12 and −5, respectively) are significantly lower (typically by a factor 10–50) than those obtained with the same catalyst for the case of $C_2H_4$ oxidation (e.g. figures 3 and 5). This is consistent

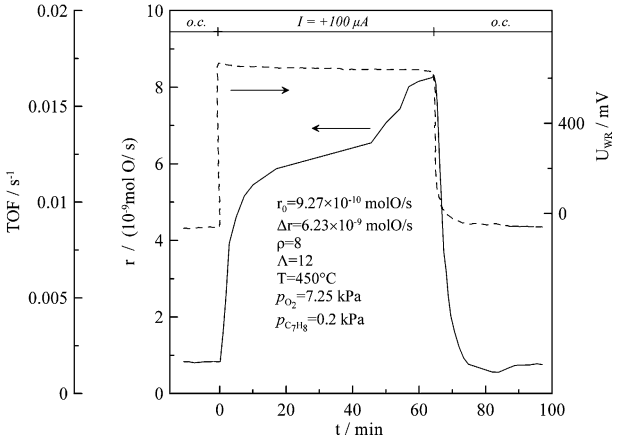


Figure 8. Transient effect of a constant anodic applied current ($I = +100$ μA) on the rate of toluene oxidation over $RuO_2$/YSZ and on the catalyst potential. $T$ = 450 °C, $P_{O_2}$ = 7.5 kPa, $P_{C_7H_8}$ = 0.2 kPa.

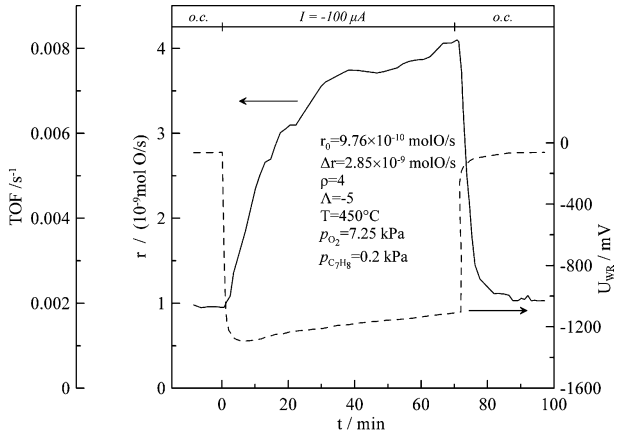


Figure 9. Transient effect of a constant cathodic applied current ($I = -100\mu$A) on the rate of toluene oxidation and on the catalyst potential. $T$ = 450 °C, $P_{O_2}$ = 7.5 kPa, $P_{C_7H_8}$ = 0.2 kPa.

with the observed significantly lower (again typically by a factor of 10–50) open-circuit rate, $r_0$, of the oxidation of toluene versus ethylene on the $RuO_2$Catalyst surface in conjunction with the equation [13,14]:

$$|\Lambda| = 2Fr_0/I_0 \qquad (10)$$

where $I_0$ is the exchange current of the $RuO_2$/YSZ interface, which predicts the magnitude of the Faradaic efficiency $\Lambda$, in electrochemical promotion studies [13,14]. Thus $\Lambda$ in the case of toluene oxidation is smaller than in the case of ethylene oxidation because the open-circuit catalytic activity, $r_0$, is smaller for toluene oxidation than for ethylene oxidation.

The peculiar rate transient of figure 8 and the observed second rate increase after 40 min of positive current application provides an indication that the

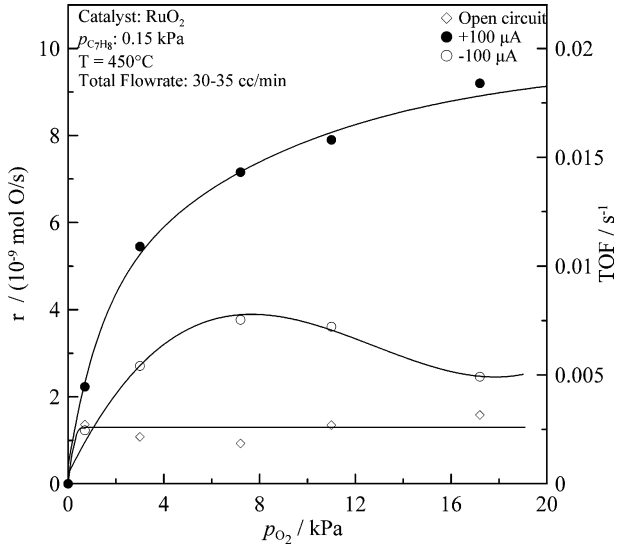


Figure 10. Dependence of the rate of toluene oxidation over $RuO_2$/YSZ on the Oxygen partial pressure under open circuit and under anodic (positive) and negative (cathodic) polarization.

catalyst surface changes from the oxide form to a partly reduced surface ($RuO_x$, $x < 2$). This is also supported by the observed gradual potential decrease during the galvanostatic transient (figure 8).

Figure 10 shows the rate dependence on $P_{O_2}$. For open-circuit and also for positive polarization, the rate is positive order in $P_{O_2}$ and this in conjunction with the observed positive order dependence on $P_{C_7H_6}$ leads to inverted volcano type behaviour, i.e. the rate is enhanced with both positive and negative potential (figure 10). Note that anodic polarization increases the reaction order with respect to $P_{O_2}$ while cathodic polarization decreases it leading eventually to negative order dependence at higher $P_{O_2}$ values (figure 10). This is consistent with the promotional rules [33] and with the weakening/strengthening of the metal-oxygen chemisorptive bond upon increasing/decreasing the catalyst potential [14,33].The appearance of a rate maximum under cathodic polarization (figure 10) indicates competitive adsorption of toluene and oxygen on the catalyst surface.

Figure 11 shows the dependence of the catalytic rate and of the current on catalyst potential. As already noted, the reaction rate exhibits inverted volcano behaviour, with a stronger electrophobic component due to the stronger chemisorption of oxygen on the catalyst surface. The Λ values corresponding to figure 11 are presented in figure 12. The measures Λ are generally lower than in the case of ethylene oxidation on the same surface (figure 5) as already discussed.

### 3.3. Mechanistic consideration

The previous discussion and application of the electrochemical promotion rules [14,33] to rationalize the observed electrochemical promotion behaviour of ethylene and toluene oxidation on $RuO_2$ has assumed implicitly a Langmuir–Hinshelwood type catalytic mechanism involving as a rate limiting step the surface reactions between adsorbed hydrocarbon intermediates [41] and adsorbed atomic oxygen (O) originating from gaseous $O_2$ adsorption. Since $RuO_2$ is a stable metallic type oxide [14,35–38], it was implicitly assumed that lattice oxygen does not participate to any significant extent to the catalytic reaction mechanism and that the electrochemically supplied promoting backspillover oxygen species $O^{\delta-}$ (most likely $O^{2-}$ [14]), which is distinct from the more covalently bonded gas supplied atomic Oxygen (O), migrate over the entire $RuO_2$

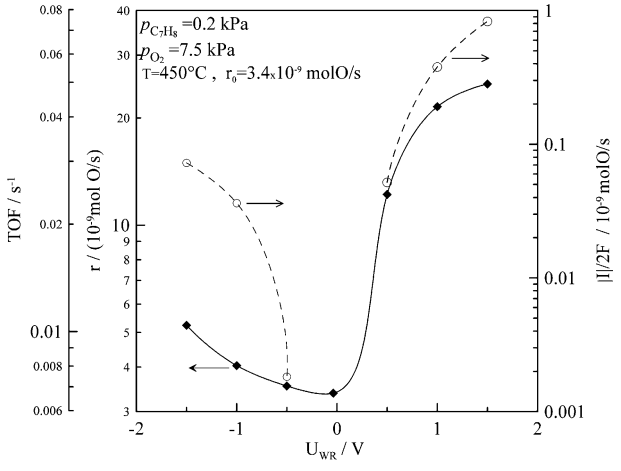


Figure 11. Effect of catalyst potential on the rate of toluene oxidation over $RuO_2$/YSZ and on the corresponding current.

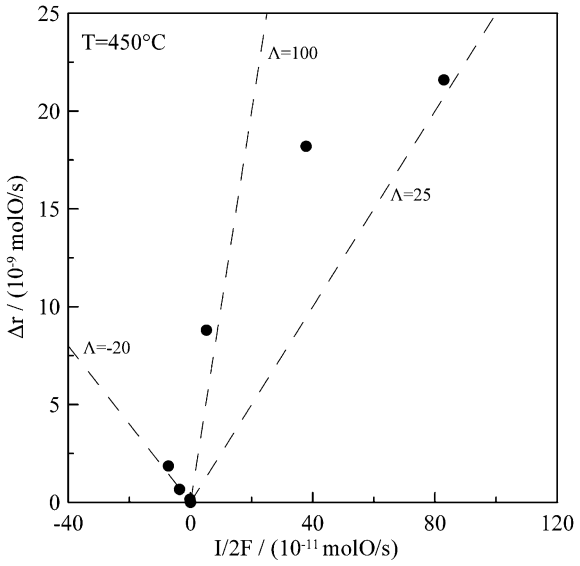


Figure 12. Effect of the applied current, $I$, on the rate of toluene oxidation over $RuO_2$/YSZ. $P_{C_7H_8}$ = 0.2 kPa, $P_{O_2}$ = 7.5 kPa.

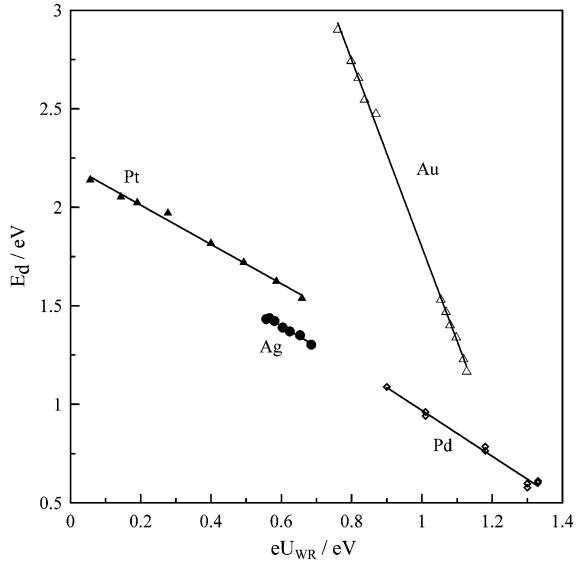


Figure 13. Effect of catalyst potential on the oxygen desorption activation energy, $E_d$, calculated from the modified Redhead analysis of $O_2$ TPD spectra from Pt, Ag, Au and Pd electrodes deposited on YSZ [14,42].

Catalyst/gas interface as they do in the case of noble metal catalyst films interfaced with YSZ establishing there an effective double layer at the catalyst/gas interface (figure 1).

It is well established that these electrochemically supplied backspillover $O^{\delta-}$ ions exert strong lateral repulsive interactions to coadsorbed atomic oxygen (O), thus causing a very pronounced and often linear decrease in the chemisorptive bond strength of atomic oxygen [14,42] (figure 13). As shown in figure 13, for the case of Pt, Ag and Pd catalyst-electrodes deposited on YSZ, the chemisorptive binding energy of atomic O decrease linearly and in fact with a slope very near to −1 with increasing catalyst potential and work function. It is this linear variation in binding energy with $eU_{WR}$ and $\Phi$ which causes the common exponential dependence of catalytic oxidation rates on $eU_{WR}$ and $\Phi$ (equation (7)). The recently developed Frumkin-type effective double-layer isotherms [14,43] provide a firm justification for the observed linear variations in heats of adsorption with $eU_{WR}$ and $\Phi$ [14,43]. It is worth noting in figure 13 that even in the case of Au which can adsorb oxygen at very positive applied potentials [44] the heat of adsorption decreases linearly, with a slope near −4 [14,44], with potential and work function.

When the metal under consideration forms surface oxides, as e.g. in the case of surface $Rh_2O_3$ formation on Rh [14,39,40] then the repulsive lateral interactions between the electochemically supplied $O^{\delta-}$ species and the oxygen atoms of the surface oxide lead to destabilization of the surface oxide and thus to very pronounced electrophobic NEMCA behaviour, as the reduced metal catalyst (e.g. Rh) is much more active for oxidation [14,39,40].

The present results (e.g. the peculiar $U_{WR}$ behaviour in figures 3, 8, 9) suggest that a similar partial surface reduction of $RuO_2$ (reaction (6)) may be taking place under anodically imposed $O^{\delta-}$ migration to the catalyst surface. *In situ* work function measurements of electropromoted $RuO_2$ [37] and $IrO_2$ Catalysts [45] have indeed confirmed the electrochemically induced $O^{\delta-}$ backspillover over the entire $RuO_2$ and $IrO_2$ surface but *in situ* surface spectroscopic characterization, as in the case of Pt [23], will be necessary to determine the exact oxidation state of the $RuO_2$ Catalyst under electropromoted conditions.

## Conclusions

$RuO_2$ polycrystalline films deposited on YSZ solid electrolyte can be effectively electrochemically promoted for the complete oxidation of volatile organic compounds (VOCs). The rate of ethylene oxidation can be increased by a factor of ten via anodic polarization and by a factor of three via cathodic polarization. The rate of toluene oxidation can be enhanced by a factor of eight via anodic polarization and by a factor of four via cathodic polarization.

Both reactions exhibit electrophobic behaviour $(\partial r/\partial U_{WR} > 0)$ at lower temperatures changing to inverted volcano behaviour above 430 °C in accordance with the kinetics and the recently found rules of electrochemical and classical promotion [14,33,43]. Under anodic polarization the $RuO_2$ state changes. It is very likely that $RuO_2$ is partly reduced to another oxide of the form of $RuO_x$, where $x < 2$. The use of surface spectroscopic methods will be useful to elucidate the electrochemically induced change in the catalyst state.

## References

[1] C.G. Vayenas, S. Bebelis and S. Ladas, Nature 343 (1990) 625.
[2] J. Pritchard, Nature 343 (1990) 592.
[3] R.M. Lambert, F. Williams, A. Palermo and M.S. Tikhov, Topics Catal. 13 (2000) 91.
[4] G. Foti, S. Wodiunig and C. Comninellis, Curr. Topics Electrochem. 7 (2000) 1.
[5] C.A. Cavalca and G.L. Haller, J. Catal. 177 (1998) 389.
[6] L. Ploense, M. Salazar, B. Gurau and E.S. Smotkin, J. Am. Ceram. Soc. 119 (1997) 11550.
[7] P. Vernoux, F. Gaillard, L. Bultel, E. Siebert and M. Primet, J. Catal. 208 (2002) 412.
[8] I. Metcalfe, J. Catal. 199 (2001) 247.
[9] C. Sanchez, E. Leiva, W. Vielstich, H. Gasteiger and A. Lamm (eds.), Handbook of Fuel Calls: Fundamentals, Technology and Applications, Vol. 2, (John Wiley and Sons Ltd., England, 2003).
[10] G.-Q. Lu and A. Wieckowski, Curr. Opin. Colloid Interf. Sci. 5 (2000) 95.
[11] B. Grzybowska-Swierkosz and J. Haber, *Annual Reports on the Progress of Chemistry*, (The Royal Society of Chemistry, Cambridge, 1994).
[12] J.O.M. Bockris and Z.S. Minevski, Electrochim. Acta 39 (1994) 1471.
[13] C.G. Vayenas, M.M. Jaksic, S. Bebelis, S.G. Neophytides, in: *Modern Aspects of Electrochemistry*, J.O.M. Bockris, B.E. Conway and R.E. White (eds), Vol. 29 (Kluwer Academic/Plenum Publishers, New York, 1996) p. 57.
[14] C.G. Vayenas, S. Bebelis, C. Pliangos, S. Brosda, D. Tsiplakides 2001 *Electrochemical Activation of Catalysis: Promotion, Electrochemical Promotion and Metal-Support Interactions*, Kluwer Academic/Plenum Publishers, New York.
[15] A. Wieckowski, E. Savinova, C.G. Vayenas (eds.), *Catalysis and Electrocatalysis at Nanoparticles*, (Marcel Dekker, Inc., New York, 2003).
[16] J. Nicole, D. Tsiplakides, C. Pliangos, X.E. Verykios, C. Comninellis and C.G. Vayenas, J. Catal. 204 (2001) 23.
[17] X.E. Verykios, in: *Catalysis and Electrocatalysis at Nanoparticles Surfaces*, A. Wieckowski, E.R. Savinova and C.G. Vayenas (eds) (Marcel Dekker, New York, 2003).
[18] C.G. Vayenas and D. Tsiplakides, Surf. Sci. 467 (2000) 23.
[19] D. Tsiplakides and C.G. Vayenas, J. Electrochem. Soc. 148 (2001) E189.
[20] C. Cavalca, G. Larsen, C.G. Vayenas and G. Haller, J. Phys. Chem. 97 (1993) 6115.
[21] C.G. Vayenas, J. Electroanal. Chem. 486 (2000) 85.
[22] I. Riess and C.G. Vayenas, Sol. St. Ionics 159(3–4) (2003) 313.
[23] S. Ladas, S. Kennou, S. Bebelis and C.G. Vayenas, J. Phys. Chem. 97 (1993) 8845.
[24] A. Palermo, M.S. Tikhov, N.C. Filkin, R.M. Lambert, I.V. Yentekakis and C.G. Vayenas, Stud. Surf. Sci. Catal. 101 (1996) 513.

[25] W. Zipprich, H.-D. Wiemhofer, U. Vohrer and W. Gopel, Berichte Bunsengesellschaft der Physikalischen Chemie 99 (1995) 1406.
[26] D. Tsiplakides and C.G. Vayenas, J. Catal. 185 (1999) 237.
[27] S. Neophytides, D. Tsiplakides, P. Stonehart, M. Jaksic and C.G. Vayenas, Nature 370 (1994) 45.
[28] D. Kek, M. Mogensen and S. Pejovnik, J. Electrochem. Soc. 148 (2001) A878.
[29] A.D. Frantzis, S. Bebelis and C.G. Vayenas, Solid State Ionics 136–137 (2000) 863.
[30] M. Makri, C.G. Vayenas, S. Bebelis, K.H. Besocke and C. Cavalca, Surf. Sci. 369 (1996) 351.
[31] C. Vayenas, D. Archonta and D. Tsiplakides, J. Electroanal. Chem. 554–555 (2003) 301.
[32] S. Bebelis and C.G. Vayenas, J. Catal. 118 (1989) 125.
[33] C.G. Vayenas, S. Brosda and C. Pliangos, J. Catal. 203 (2001) 329.
[34] C. Comninellis and G.P. Vercesi, J. of Appl. Electrochem. 21 (1991) 335.
[35] S. Wodiunig and C. Comninellis, J. Eur. Ceramic Soc. 19 (1999) 931.
[36] S. Wodiunig, F. Bokeloh and C. Comninellis, Electrochim. Acta 46 (2000) 357.
[37] S. Wodiunig, V. Patsis and C. Comninellis, Solid State Ionics 136–137 (2000) 813.
[38] S. Wodiunig, F. Bokeloh, J. Nicole and C. Comninellis, Electrochem. Solid-State Lett. 2 (1999) 281.
[39] C. Pliangos, I.V. Yentekakis, X.E. Verykios and C.G. Vayenas, J. Catal. 154 (1995) 124.
[40] E.A. Baranova, A. Thursfield, S. Brosda, G.Fóti, Ch. Comninellis, C.G. Vayenas, J. Electrochem. Soc. in press (2004).
[41] L.L. Hegedus, R. Aris, A.T. Bell, M. Boudart, N.Y. Chen, B.C. Gates, W.O. Haag, G.A. Somorjai and J. Wei, *Catalyst Design: Progress and Perspectives*, (John Wiley and sons, New York, 1987).
[42] A. Katsaounis, PhD Thesis, University of Patras (2003).
[43] S. Brosda and C.G. Vayenas, J. Catal. 208 (2002) 38.
[44] D. Tsiplakides, S.G. Neophytides and C.G. Vayenas, Ionics 7 (2001) 203.
[45] J. Nicole and Ch. Comninellis, Solid State Ionics 136–137 (2000) 687.